Retrieved Refractivity field in Southern Taiwan during SoWMEX/TiMREX Experiment

Ya-Chien Feng[1*], Tai-Chi Chen Wang[1], Tammy Weckwerth[2], Wei-Jun Chen[1]
[1] National Central University, Jhongli City, Taoyuan, Taiwan
[2] National Center of Atmospheric Research, Boulder, Colorado., USA
* Currently at McGill University, Montreal, Canada

1. Introduction

Refractivity retrieval during Southwest Monsoon Experiment/Terrain-influenced Monsoon Rainfall Experiment (SoWMEX/TiMREX 2008) provides the valuable near-surface moisture spatial distribution in tropical southern Taiwan (Fig.1). During the experiment, refractivity data were retrieved using the NCAR S-Pol radar (22.5268°N, 120.4335°E).

This retrieval technique was developed by Fabry et. al (1997) based on the concept that variability in the received phase of radar waves propagating between the radar and fixed ground targets is due to the properties of the intervening air. Refractivity (N) is related to meteorological parameters (Bean and Dutton, 1968):

$$N = 77.6\frac{P}{T} + 3.73 \times 10^5 \frac{e}{T^2}$$

The first term is related to the air density. The second term is related to moisture and temperature, and most of the spatial variation in N results from this term.

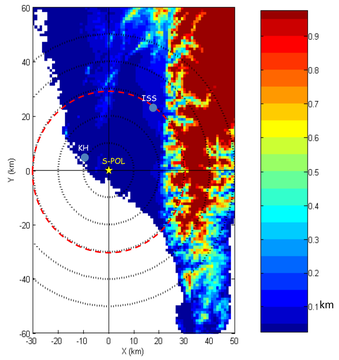

Fig. 1 Southern Taiwan Topography.

2. Data processing

The quality of the retrieval depends critically on the quality of:

- **Ground Target Identification**: The better targets are distributed from the NE-SW direction within 30 km from S-Pol. The data collected over 1.5 hours on 9 June 2008 were used to identify fixed, reliable and strong targets (Fig. 2).
- **Calibration (Reference) data**: The calibration data were collected on 4 June 2008 when the low-level atmospheric condition was near homogeneous under light stratiform rainfall. The ideal reference phase difference (Fig. 3) has minimal gradients and no folding in azimuth and range.

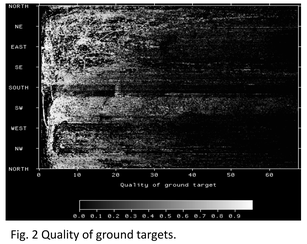

Fig. 2 Quality of ground targets.

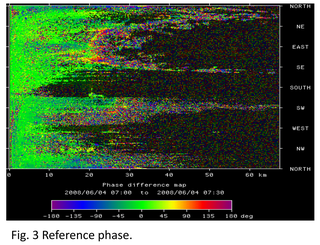

Fig. 3 Reference phase.

3. Validation

3-1 Frontal system on June 2 2008 (Fig. 4)

The refractivity (N) gradient shows consistency with the leading edge of the frontal system shown in the reflectivity field (Z). Larger (smaller) N values correspond with the high (low) reflectivity areas. As the frontal system moves, refractivity also shows the spatial variations.

3-2 Site by site comparison (Fig. 5)

The trends of radar retrieval and surface station refractivity are consistent but with small noisy values. There are some possibilities needed to be discussed.

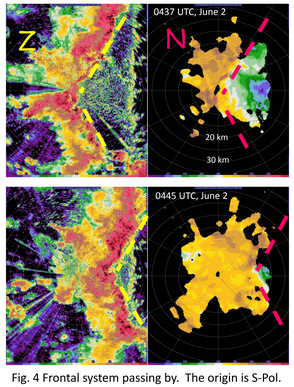

Fig. 4 Frontal system passing by. The origin is S-Pol.

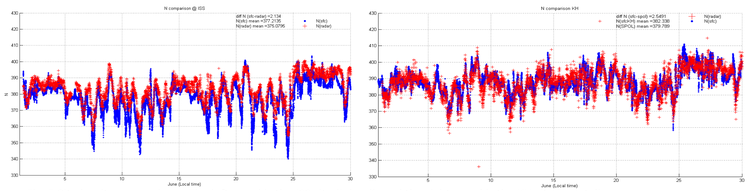

Fig. 5 Site by site comparison. The left panel is the ISS site (inland), and the right panel is the KH site (coastal).

4. Application

4-1 Non-IOP case (June 20, Fig. 6)

(a) Diurnal refractivity variation with land-sea interaction.

(b) Refractivity field shows the N-S gradient in the afternoon. Thirty minutes later, the convection initiated in the foothills in the significant refractivity gradient area.

4-2 IOP case (June 14, Fig. 7)

Even in a moisture environment, refractivity is useful to illustrate the low-level thermodynamic variability. The refractivity trend in the northern portion shows that the conditions are more unfavorable for convection with lower (drier) N values. This is consistent with the observed decaying convection. It further shows the moistening of the near-surface air from the south (after 1400 LST), which allows the convection to develop in that region.

4-3 IOP case (May 26, Fig. 8)

Consistent perceptible water(PW) observed by ground-based GPS through out the day. Moisture in foothills increased as the afternoon storm. Refractivity shows the significant outflow boundary.

5. Discussion

The value of refractivity during SoWMEX/TiMREX is between 360-410 units, which is higher than that of previous experiments on the inland plains. The variation of the N represents the significant atmospheric condition change in such high temperature and humidity tropical insular environments. In a calm non-IOP day, the diurnal variation of N inland could reach 40 units, while along coast the variation is within 20 units. From Gao et al. (2007), the N variation can be divided into two terms, a contribution from temperature(T) and a contribution from dew temperature (Td):

$$\delta N = A\delta T + B\delta Td, \quad \alpha = 17.26, \beta = 35.86$$
$$A \equiv \frac{\partial N}{\partial T} = -\left(\frac{77.6P}{T^2} + \frac{2 \times 3.73 \times 10^5 e}{T^3}\right)$$
$$B \equiv \frac{\partial N}{\partial Td} = \frac{3.73 \times 10^5 (273.16 - \beta)\alpha e}{T^2 (Td - \beta)^2}$$

For example, T= 30℃, TD = 25℃ , RH ~ 75%, A= -1.7, B=7.6, |B/A| ~ 4.5. During SoWMEX/TiMREX with a temperature range of 22 to 35℃ , ΔTd = 1℃ will result in 4 to 5 times more N variation than ΔT=1℃. With higher temperature, the influence of moisture change on N becomes significant.

The refractivity data of SoWMEX/TiMREX are valuable for providing information about the 2-D high-resolution low-level thermodynamic conditions within a tropical environment. Some cases are presented to show that the refractivity field could be monitored as possible precursor for convection initiation and development, especially when there are low-level thermodynamic boundaries, such as gust fronts and sea-breeze fronts.

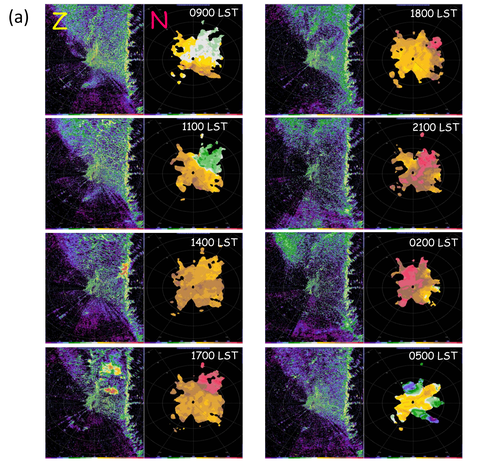

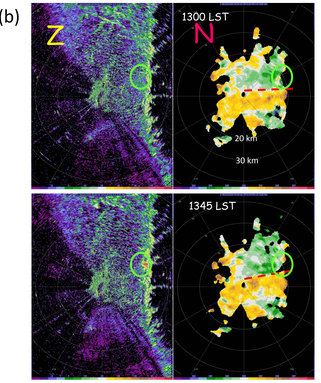

Fig. 6 Non-IOP case on June 20:
(a) Diurnal variation of reflectivity (Z) and refractivity (N).
(b)Refractivity field shows the gradient indicating the different atmospheric conditions before a convection initiation event.

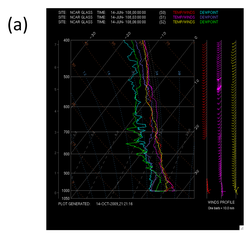

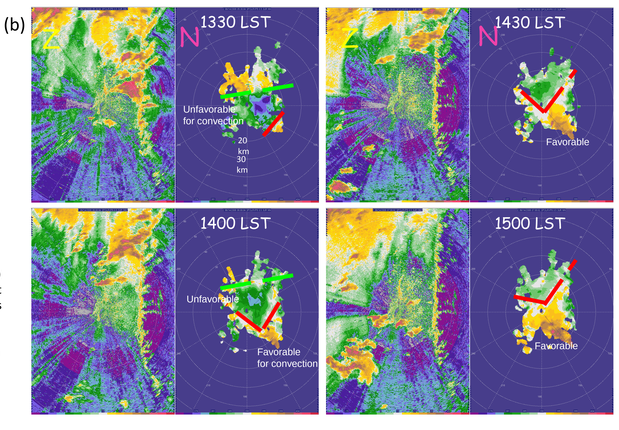

Fig. 7 IOP case on June 14.
(a) Sounding data (b) Refractivity field (N) from 1330 to 1500 LST shows the gradient indicating the unfavorable (lower N values propagating northward shown by green dashed line) and favorable (higher N values propagating from the south shown by red dashed line) environments for convective development.

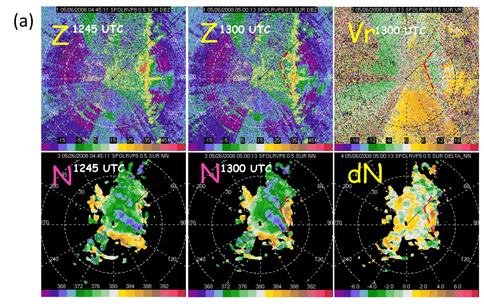

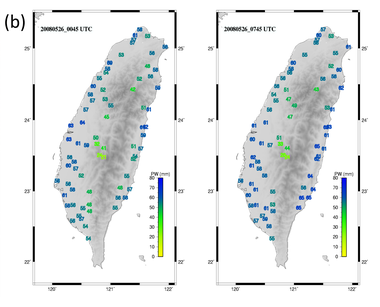

Fig. 8 IOP case on May 26.
(a) Temporal various of reflectivity (Z) and refractivity (N) within 15 mins. Refractivity field shows the outflow boundary (shown in red dash) which also can be found in Vr (radial wind field) and delta N (dN) field. (b) Perceptible water (PW) measured by ground-based GPS receivers.

Reference

Bean, B. R., and E. J. Dutton, 1968: *Radio Meteorology*. Dover Publications, 435 pp.

Fabry, F., C. Frush, I. Zawadzki, and A. Kilambi, 1997: On the extraction of near-surface index of refraction using radar phase measurements from ground targets. *J. Atmos. Oceanic Technol.*, **1**, 978–987.

Gao, J. D., K. Brewster, and M. Xue, 2008: Variation of radio refractivity with respect to moisture and temperature and influence on radar ray path. *Adv. Atmos. Sci.*, **25**(6), 1098–1106, doi: 1007/s00376-008-1098-x.

Acknowledgements

Surface station data were obtained from Pay-Liam Lin (NCU) and Ching-Hwang Liu (CCU). We appreciate thoughtful and enlightening discussions with Frédéric Fabry (McGill), Scott Ellis (NCAR), Rita Roberts (NCAR), Jason Fritz (CSU) and Eric Nelson (NCAR).